Supporting Information

Electrophilic N, P Co-Doped Carbon Enabling Highly Reversible Iodine Redox Chemistry for Ultra-Stable Bismuth-Based Zinc-Ion Batteries

*Dandan Ling,[a] Yan Ma,[a] Liu Jiang,[a] Tong Zhou,[*b,d] Daohong Zhang,[*a,c] Qiufan Wang[*a,c]*

[a] Key Laboratory of Catalysis and Energy Materials Chemistry of Ministry of Education & Hubei Key Laboratory of Catalysis and Materials Science, Hubei R&D Center of Hyperbranched Polymers Synthesis and Applications, South-Central Minzu University, Wuhan 430074, China

[b] Hubei Key Laboratory of Energy Storage and Power Battery, School of New Energy, Hubei University of Automotive Technology, Shiyan 442002, China

[c] Guangdong Provincial Laboratory of Chemistry and Fine Chemical Engineering Jieyang Center, Jieyang 515200, China

[d] Key Laboratory of Advanced Energy Materials Chemistry, Nankai University, Tianjin 300071, China

Email: zhoutong1018@huat.edu.cn (T. Zhou); daohong.zhang@scuec.edu.cn (D. Zhang); ygdf@mail.scuec.edu.cn (Q. Wang)

Experimental section

Synthesis of Bi-BTC: 0.09 g Bi $(NO_3)_2 \cdot 5H_2O$ and 0.45 g H_3BTC were dissolved in 60 mL MeOH and stirred for 30 min. Subsequently, the obtained transparent solution was transferred to a 100 mL Teflon-lined stainless steel autoclave and kept at 120 ℃ for 24 h. After cooling to room temperature, the obtained product was washed several times with MeOH and collected by centrifugation. Subsequently, the product was dried in vacuum at 60 ℃ overnight to obtain white Bi-BTC powder.

Synthesis of Bi-BTC@PANI：200 mg Bi-BTC powder was ultrasonically dispersed in 100 mL of deionized water. Dissolve 300 μL aniline in 5 mL deionized water, and then drop it into Bi-BTC solution in ice-bath. Dissolve 844 mg of ammonium thiosulfate in 5 mL of deionized water, drop it into the mixed solution in ice-bath, and keep stirring for 2 h. Washing with deionized water for several times by vacuum filtration, and then vacuum drying at 80 ℃ for 12 h to obtain Bi-BTC@PANI.

Synthesis of Bi@C, Bi@NC and Bi@NPC: A ceramic boat containing Bi-BTC@PANI was placed at the downstream side of a tube furnace, while NaH_2PO_2 was positioned upstream (mass ratio of Bi-BTC@PANI to NaH_2PO_2=1:1). The temperature was raised to 600 °C at a heating rate of 5 °C min^{-1} and maintained for 3 h under an Ar atmosphere to obtain Bi@NPC. For comparison, Bi-BTC@PANI powder was calcined at 600 °C for 3 h under Ar without NaH_2PO_2 to produce Bi@NC. The pristine Bi-BTC without any pretreatment was directly subjected to the same calcination conditions to yield Bi@C.

Characterization:

The synthesized sampled were characterized by X-ray powder diffraction (XRD) and X-ray photoelectron spectroscopy (XPS). The morphology and structure of the samples were characterized by scanning electron microscopy (SEM) and transmission electron microscopy (TEM). The bond structures were described by Raman and FTIR spectra. The specific surface area and pore volume were determined by measuring nitrogen adsorption/desorption isotherms. The UV–vis measurements were carried out using a quartz cuvette with a path length of 1 cm, and the sample concentration was adjusted to ensure an absorbance within the linear range.

Electrochemical measurement:

The sample, Super P and PVDF were mixed in NMP solvent according to the mass ratio of 7:2:1, then the slurry was evenly coated on carbon cloth (CC) and dried in vacuum at 60 ℃ for 12 h. The electrochemical evaluation was carried out by assembling into a CR2032-type coin cell, using Zn foil as anode, glass fiber as separator, 2 M $ZnSO_4$ and 0.2 M KI as electrolyte, respectively. The galvanostatic charge/discharge (GCD) measurements were carried out with Neware Battery Tester (BTS-4000) in the voltage window of 0.1-1.6 V (vs Zn^{2+}/Zn). Cyclic voltammetry (CV) and electrochemical impedance spectroscopy (EIS) were tested on IVium 10800 electrochemical workstation.

Detail of calculation

(1) Capacitance contribution

the measure current (*i*) and scan rate (*v*) in CV curves have relationships with equation:

$$i=a^{v}b \tag{1}$$

$$logi=blogv+loga \tag{2}$$

Where *a* denotes a constant, *b* is equal to the slope of *lgv-lgi* plots, *i* represents peak current, *v* is the scan rate of CV curve. When the value of *b* is close to 0.5, the electrode shows a diffusion process, and when the value of *b* is close to 1, the capacitance process is dominant.

Capacitance contribution can be further calculated according to the equations:

$$i(v)=k_1v+k_2v^{1/2} \tag{3}$$

$$i(v)/v^{1/2}=k_1v^{1/2}+k_2 \tag{4}$$

Where k_1 value was obtained from the slope of linear fit of the $i/v^{1/2}$ versus $v^{1/2}$ plot. The capacitive and diffusion-controlled contributions were obtained by k_1v and $k_2v^{1/2}$, respectively.

(2) Calculation details

All spin-polarized DFT calculations were performed using CASTEP code with the Perdew-Burke-Ernzerhof (PBE) functional of generalized gradient approximation (GGA).[1, 2] The DFT-D3 was used to describe the dispersion interaction for correcting the long-range van der Waal's interactions.[3] The cut-off energy for the plane-wave

basis was set to 500 eV, and k points were sampled with 3×3×1 Monkhorst-Pack mesh. Moreover, the energy and force convergence thresholds were set to 10^{-5} eV/atom and 0.03 eV/Å, respectively. All samples were modeled as slabs based on a 6×6 supercell of graphene with a 15 Å-thick vacuum layer between adjacent monolayers in the z direction. In specifically, the computational model for NC contains three kinds of doping N species, i.e., pyrrolic, pyridinic and graphitic N with the ration of 2: 3: 1, which is consistent with the XPS results. In addition, based on the experimental analyses that indicate the nonexistence of P-N bonds and the present of P-C bonds in NPC, we explored the different P-doped sites and identified the theoretical model in the lowest-energy configuration (Figure S18). The Gibbs free energy for each elementary step of iodine reduction reaction was calculated using the CHE model at 298.15 K. Briefly, $\Delta G=\Delta E+T\Delta S+\Delta EZPE+\Delta\int CpdT$, in which ΔE, $\Delta EZPE$, ΔS, and $\Delta\int CpdT$ denote the differences of the electronic energy, zero-point energy (ZPE), entropy, and heat capacity between reactants and production in elementary reaction step, respectively.

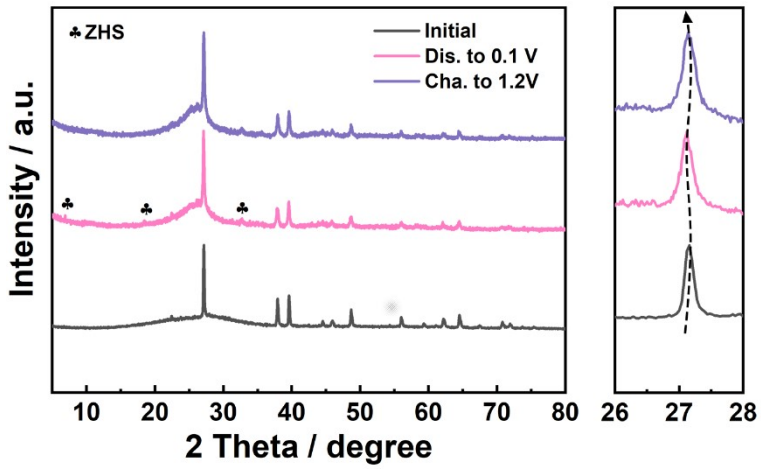

Figure S1. XRD pattern of Bi@NPC electrode in 2 M $ZnSO_4$ electrolyte during charging and discharging.

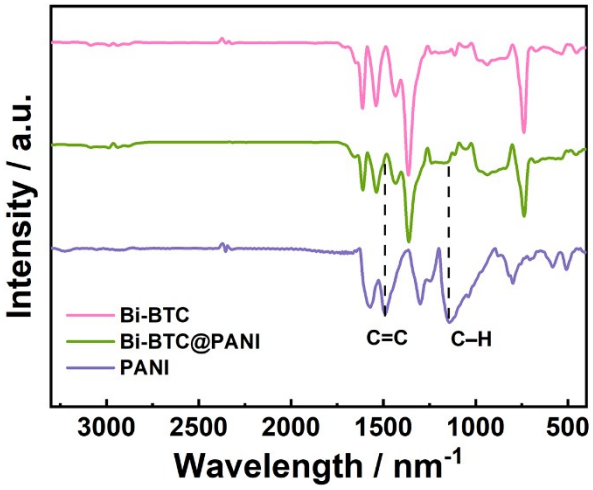

Figure S2. FTIR spectra of Bi-BTC, Bi-BTC@PANI and PANI.

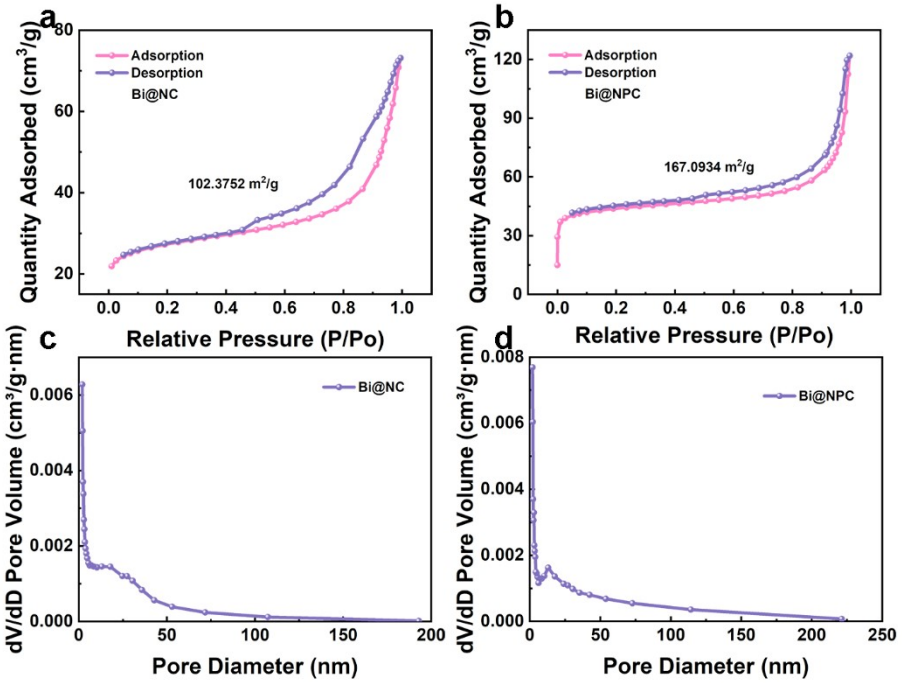

Figure S3. N_2 adsorption-desorption isotherms and pore size distribution (inset) of Bi@C and Bi@NC.

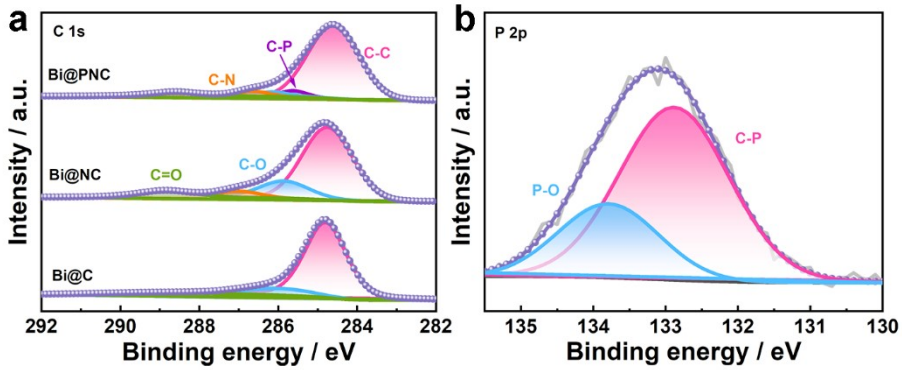

Figure S4. (a) C 1s XPS spectra of Bi@C, Bi@NC and Bi@NPC. (b) P 2p XPS spectrum of Bi@NPC.

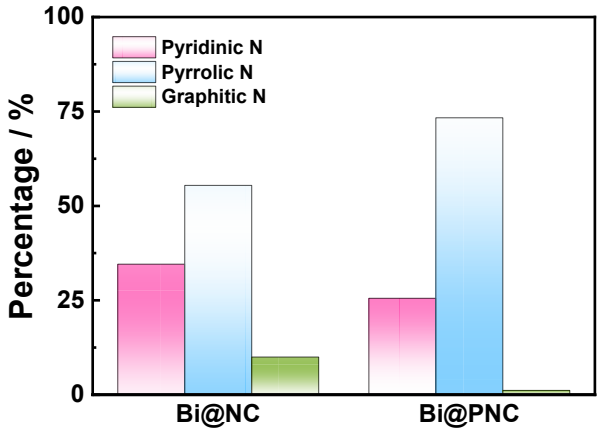

Figure S5. Percentage of peak areas of various N species in Bi@NC and Bi@NPC.

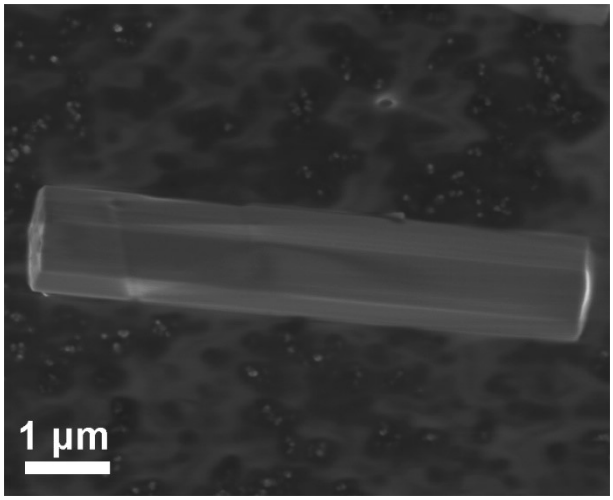

Figure S6. SEM image of Bi-BTC.

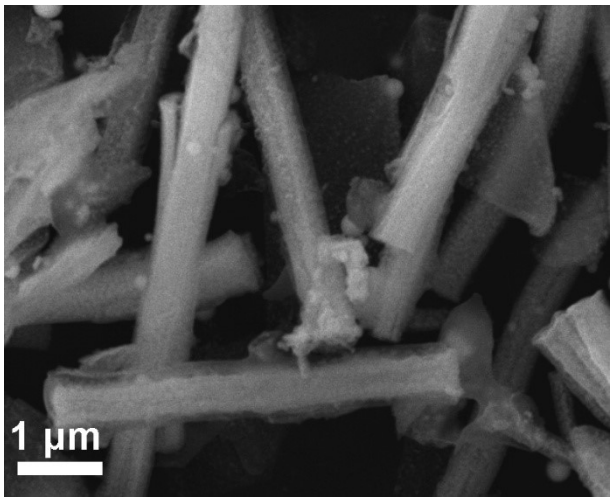

Figure S7. SEM image of Bi@NPC.

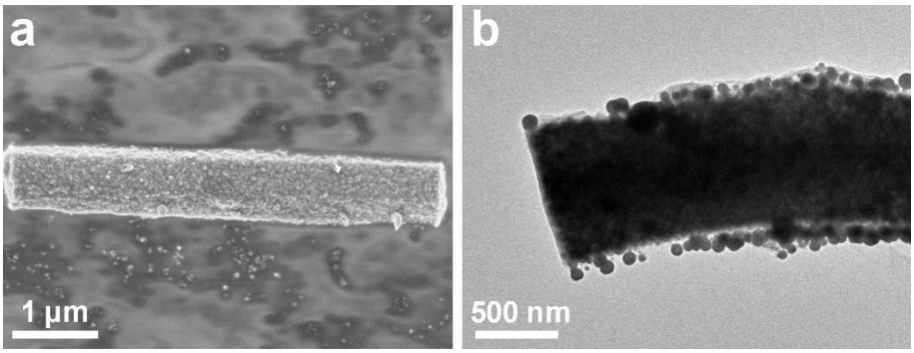

Figure S8. (a) SEM and (b) TEM images of Bi@C.

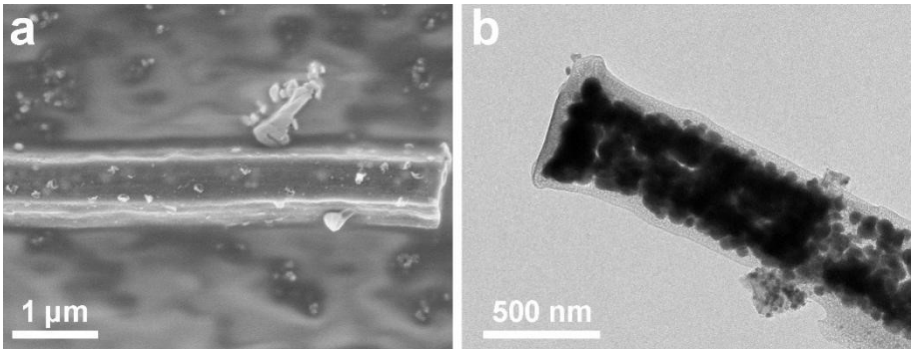

Figure S9. (a) SEM and (b) TEM images of Bi@NC.

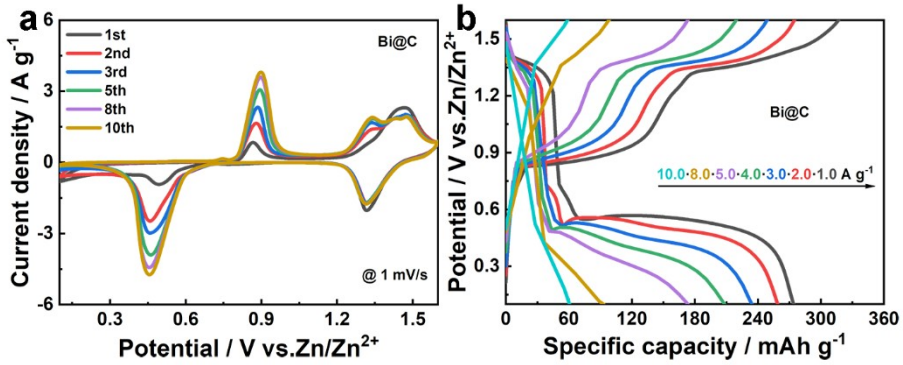

Figure S10. Electrochemical properties of Bi@C: (a) CV and (b) GCD curves.

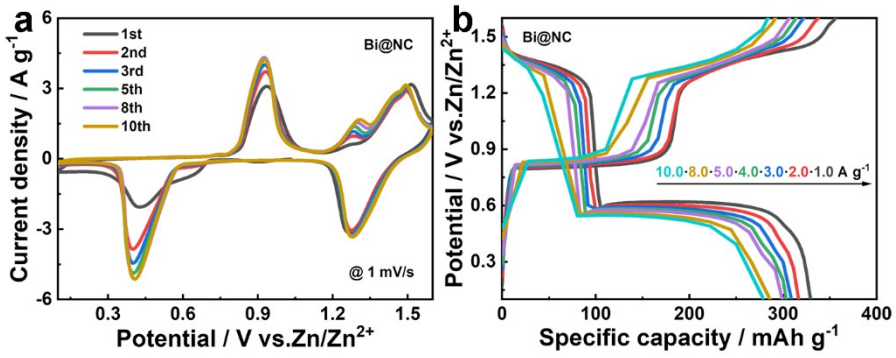

Figure S11. Electrochemical properties of Bi@NC: (a) CV and (b) GCD curves.

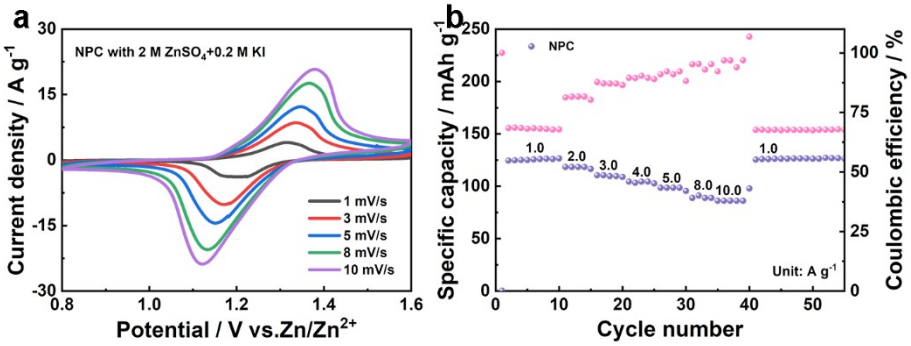

Figure S12. Electrochemical properties of NC with 2 M $ZnSO_4$+0.2 M KI: (a) CV curves and (b) rate performance.

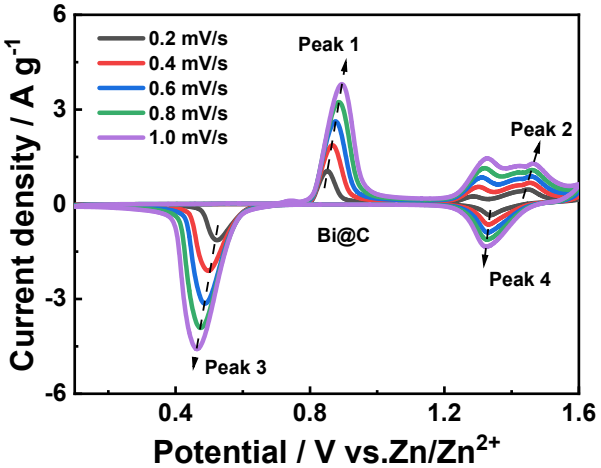

Figure S13. CV curves of Bi@C electrode at scan rates from 0.2 to 1.0 mV s^{-1}.

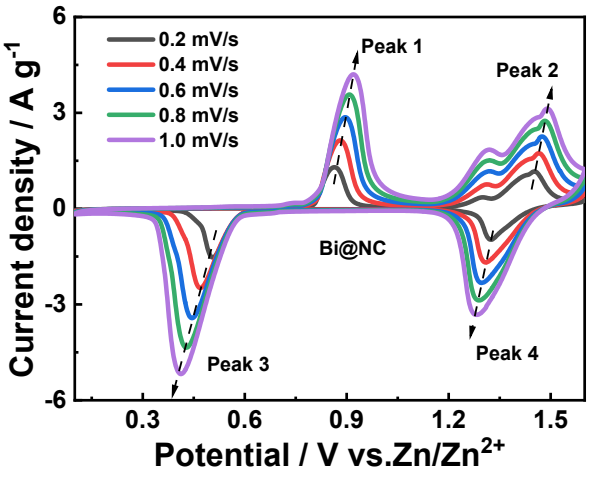

Figure S14. CV curves of Bi@NC electrode at scan rates from 0.2 to 1.0 mV s^{-1}.

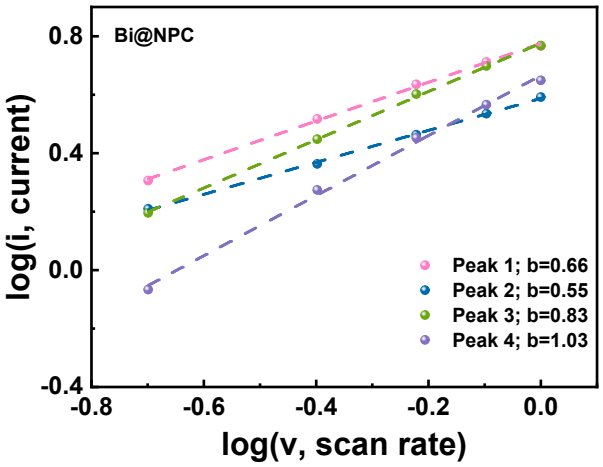

Figure S15. Log *i* vs log *v* plots at specific peak currents.

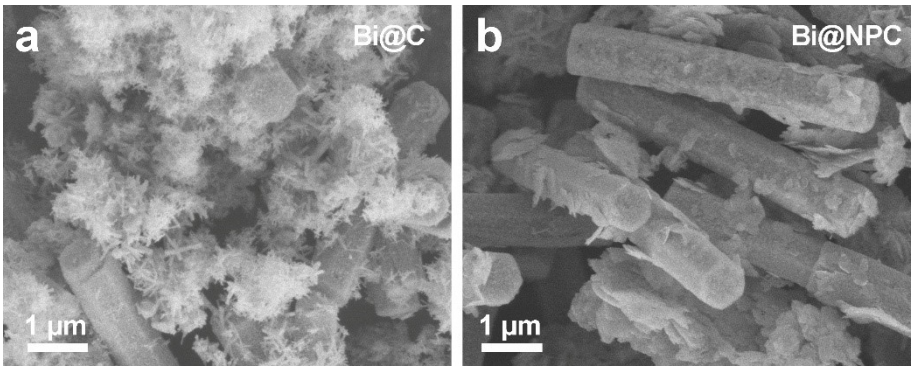

Figure S16. SEM images of Bi@C and Bi@NPC electrodes after cycling.

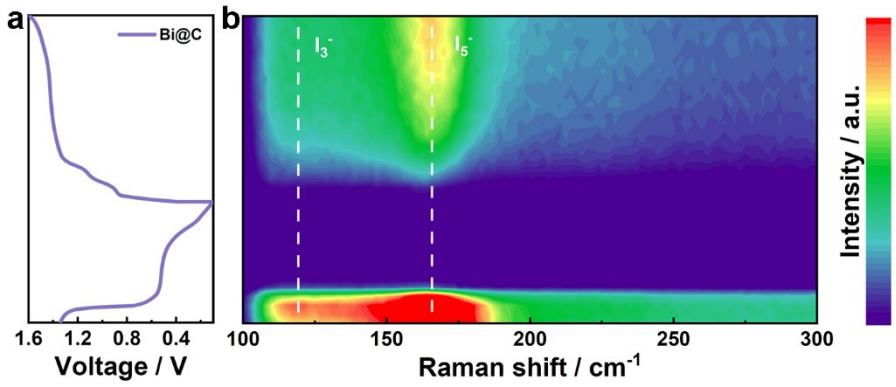

Figure S17. (a) GCD curve and (b) corresponding *in situ* Raman spectra of Bi@C.

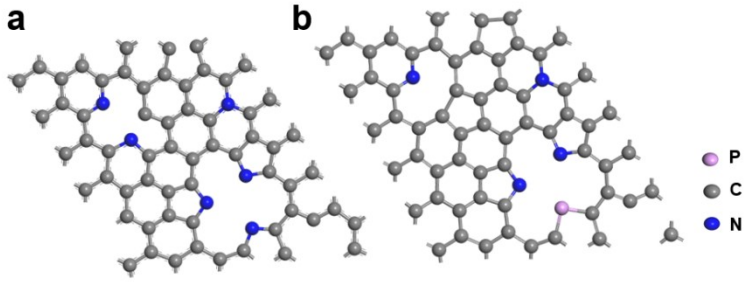

Figure S18. Models of N-doped carbon and N,P co-doped carbon.

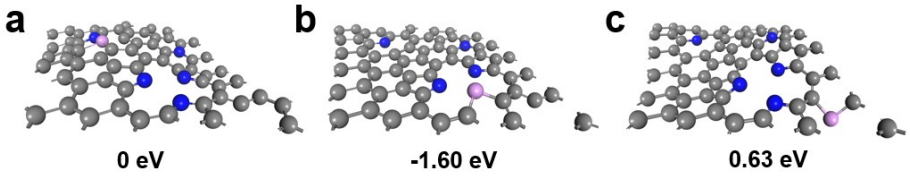

Figure S19. Optimized geometric configuration and relative energy of NPC.

References

[1] M. Segall, P. Lindan, M. Probert, C. Pickard, P. Hasnip, S. Clark, M. Payne, *J. Phys.: Condens. Matter* **2002**, *14*, 2717–2744.

[2] J. Perdew, M. Ernzerhof, K. Burke, *J. Chem. Phys.* **1996**, *105*, 9982–9985.

[3] A. Tkatchenko, M. Scheffler, *Phys. Rev. Lett.* **2009**, *102*, 073005.